Double Core-Hole Creation by Sequential Attosecond Photoionization

Kenji Tamasaku,[1,*] Mitsuru Nagasono,[1,†] Hiroshi Iwayama,[2] Eiji Shigemasa,[2] Yuichi Inubushi,[1] Takashi Tanaka,[1] Kensuke Tono,[3] Tadashi Togashi,[3] Takahiro Sato,[1] Tetsuo Katayama,[3] Takashi Kameshima,[3] Takaki Hatsui,[1] Makina Yabashi,[1] and Tetsuya Ishikawa[1]

[1]*RIKEN SPring-8 Center, 1-1-1 Kouto, Sayo-cho, Sayo-gun, Hyogo 679-5148, Japan*
[2]*UVSOR Facility, IMS, 38 Nishigo-Naka, Myodaiji-cho, Okazaki-shi, Nagoya 444-8585, Japan*
[3]*JASRI, 1-1-1 Kouto, Sayo-cho, Sayo-gun, Hyogo 679-5198, Japan*

(Received 10 April 2013; published 23 July 2013)

X-ray fluorescence spectroscopy demonstrates that a single core-hole krypton with a 170-as lifetime can be photoionized again to a double core-hole state by an intense x-ray pulse. The observation indicates that unconventional interaction between intense x rays and atoms is no more negligible in applications with x-ray free-electron lasers. Quantitative analysis of the double core-hole creation including effects of a pulsed and spiky temporal structure enables estimation of the x-ray pulse duration in the sub-10-fs range.

DOI: 10.1103/PhysRevLett.111.043001 PACS numbers: 32.80.Fb, 41.50.+h, 42.65.−k

Intense femtosecond x rays from free-electron lasers (FELs) [1,2] open up novel opportunities in diffractometry, such as the diffract-before-destroy scheme in protein crystallography [3–6]. On the other hand, conventional x-ray crystallography is based on the assumption that the scattering atoms are in the ground state. It is not trivial whether the assumption is still valid for intense x rays from FEL. Recently, it has been shown that intense soft x rays can strip all of the electrons from a neon atom [7,8]. Although hard x rays interact with atoms less strongly than soft x rays do, the scattering process by intense hard x rays might also enter the unexplored regime where excited atoms with core holes also act as scatterers in a molecule or a crystal.

The scattering properties of atoms are considered to change drastically [9,10], when incident x rays photoionize a $1s$ (K-shell) electron. The well-localized K shell dominates the reflection intensities at higher scattering angles, and the absence of a K-shell electron may limit the achievable spatial resolution in structural analysis. The creation of a core hole in the K shell shifts the absorption edge to a higher energy and is predicted to suppress anomalous dispersion [11], which could have a significant effect on solving the phase problem in single- or multiwavelength anomalous diffraction [12]. Thus, experimental study on the core-hole states is of crucial importance for x-ray nonlinear optics as well as x-ray FEL applications. The first and inevitable step is to observe x-ray interaction with core-hole states and to understand the process quantitatively.

In this Letter, we report the first observation of the double core-hole (DCH) creation by sequential hard x-ray photoionization. We measure x-ray fluorescence from krypton atoms to investigate core-hole states, while the soft x-ray DCH observation used the charged particle spectroscopy [7,13,14]. The fluorescence spectroscopy is feasible and becomes efficient for medium-Z atoms due to higher fluorescence yield. Figure 1 illustrates the initial processes in atoms excited by intense x rays. The x-ray fluorescence by F_1 and F_2 provides valuable information, such as the numbers of neutral and single core-hole (SCH) atoms interacting with x rays. Observation of F_2 gives direct evidence of x-ray interaction with the SCH atoms. In addition, we analyze quantitatively P_1 and P_2 and estimate the pulse duration in the sub-10-fs range.

The advantage of choosing krypton as the target is twofold. First, krypton is a monoatomic gas and frees us from the complexity of the two-site DCH state [13,14]. Second, krypton lies in the fourth row of the periodic table, two places from selenium, which is widely used for the anomalous phasing in protein crystallography by substituting for sulfur in amino acids [15]. Studies of krypton thus provide a benchmark for evaluating the nonlinear response of selenium.

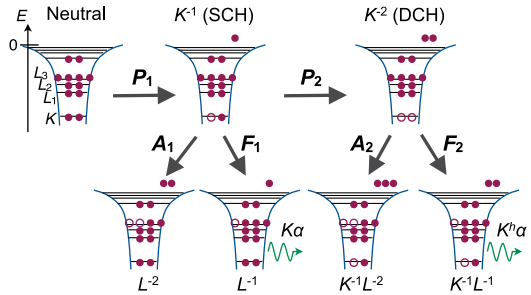

FIG. 1 (color online). Schematic diagram of x-ray photoionization and decay processes in krypton. A 15-keV x-ray photon creates an SCH atom by photoexciting the K electron (P_1). The SCH state decays with a 170-as lifetime by emitting x-ray fluorescence (F_1) or the nonradiative Auger process (A_1), ejecting another electron. Intense x rays can excite the remaining K electron before decay (P_2), producing a DCH atom with two K holes. The DCH state decays by F_2 or A_2. Minor or higher-order processes are not shown.

X-ray laser pulses from SACLA [2] were focused by a Kirkpatrick-Baez mirror system [16] into a gas cell filled with krypton at the atmospheric pressure. The central photon energy was 15.0 keV, just above the threshold of P_2 in Fig. 1, 14.874 keV [17], and the full-width-at-half-maximum (FWHM) bandwidth was about 40 eV. The focal spot was an ellipse with diameters of 1.2 and 1.3 μm (FWHM) as measured by knife-edge scans. The pulse energy of each shot was recorded by a calibrated thin-film monitor. X-ray fluorescence spectra were measured by scanning a bent crystal analyzer with the Ge 220 reflection in the Johannson geometry. The analyzer was set at a right angle to the x-ray beam within the polarization plane to suppress elastic x rays, and covered a solid angle of 6.4×10^{-3} sr for the spectrum measurement. An MPCCD (multiport charge-coupled device) with a fast readout capability and a single-photon sensitivity was used to count the x-ray fluorescence shot by shot. The photon-energy resolution of the spectrometer was estimated to be about 10 eV.

Figure 2 shows x-ray fluorescence spectra of krypton measured at two different x-ray intensities. The average pulse energies (the range of pulse energy) for high and low intensity pulses were 80.2 μJ (74.6–88.6 μJ) and 49.9 μJ (42.0–56.0 μJ), respectively. Two prominent peaks correspond to $K\alpha$ lines, which are the x-ray fluorescence from the SCH state (F_1 in Fig. 1). The higher intensity peak is $K\alpha_1$, corresponding to transitions from the L_3 subshell to the K shell, while the other is $K\alpha_2$ ($L_2 \rightarrow K$).

Another set of peaks is observed on the tail of the high-energy side of the spectrum measured at high x-ray intensity and is assigned to hypersatellites (F_2 in Fig. 1), which are x-ray fluorescence from the DCH states [18]. It is surprising that a single x-ray pulse can create the DCH krypton because two x-ray photons have to photoionize the same atom with about a 1-Å diameter within the SCH lifetime, which is only 170 as [19]. The hypersatellite peaks are denoted as $K^h\alpha_1$ and $K^h\alpha_2$ in the same order as $K\alpha_1$ and $K\alpha_2$. The photon-energy shifts of $K^h\alpha_{1,2}$ relative to $K\alpha_{1,2}$ are due to the weaker Coulomb screening in the DCH state and are measured to be 380 ± 5 and 376 ± 5 eV, respectively. The observed shifts are about 10 eV smaller than the theoretical calculation [20]; however, the photon-energy resolution is insufficient for the detailed discussion. No clear hypersatellite peak is observed for the spectrum measured at low x-ray intensity, implying a nonlinear dependence of $K^h\alpha$ on the x-ray intensity.

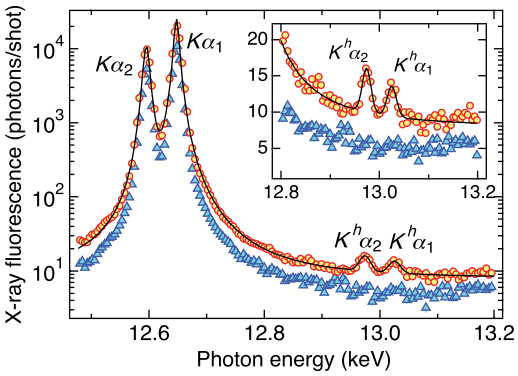

FIG. 2 (color online). X-ray fluorescence spectra of krypton. The circles and triangles were measured with high and low intensity x rays, respectively. The solid line is the fitting with the Pearson VII function. The inset shows the magnified spectra around the hypersatellites. The vertical bar on each point indicates the standard error of the mean.

We discuss here briefly the intensity ratio between $K^h\alpha_1$ and $K^h\alpha_2$, which relates to the atomic model, such as the coupling of the angular momenta [21]. To estimate the background by $K\alpha$ lines, the spectrum is fitted by the Pearson VII function [22]. Then, the ratio is found to be $I(K^h\alpha_1)/I(K^h\alpha_2) = 0.70 \pm 0.06$, which indicates the intermediate coupling for krypton ($Z = 36$) and to be slightly lower than the theoretical calculations of 0.772 [20] and 0.803 [23]. Detailed studies of the ratio in krypton could serve as a test of theoretical calculations and the atomic model, since the Z dependence of the ratio is steep around $Z = 36$ [23].

It is important to check the x-ray pulse-energy dependence of the DCH creation to rule out one-photon mechanisms [24,25], such as shakeoff by the second-harmonic radiation of FEL. Figure 3 shows the fluorescence intensities at the $K\alpha_1$ and the $K^h\alpha_2$ peaks as a function of the pulse energy. The pulse energy was controlled by attenuators made of silicon plates with various thicknesses. The pulse-energy dependence for $K\alpha_1$ is linear as expected, while that for $K^h\alpha_2$ is superlinear. As shown in Fig. 3(b), the dependence for $K^h\alpha_2$ is explained as a sum of linear

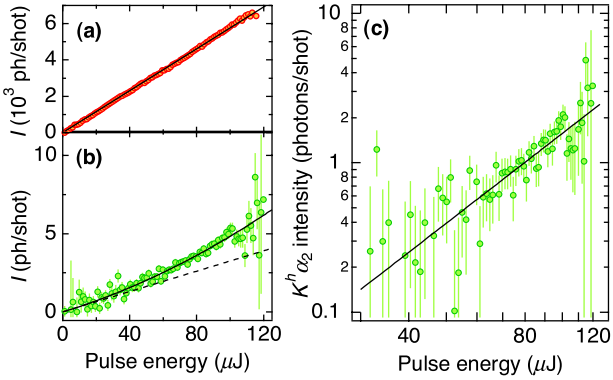

FIG. 3 (color online). Pulse-energy dependence of fluorescence intensity. (a) Measured on the $K\alpha_1$ peak. The solid line is a linear fit. (b) Measured on the $K^h\alpha_2$ peak. The solid line is a fit with a sum of linear and quadratic terms, and the dashed line shows the linear part. (c) The pulse-energy dependence of the $K^h\alpha_2$ intensity deduced by subtracting the linear component of (b). The solid line with a slope of two is the quadratic term of the fit. The vertical bar on each point in (b) and (c) indicates the standard error of the mean.

and quadratic terms, where the linear term represents the contribution from the tail of the $K\alpha$ lines (Fig. 2). The net $K^h\alpha_2$ intensity estimated by subtracting the linear term shows quadratic dependence expected for the two-photon process [Fig. 3(c)]. We note that the fluorescence intensity of Fig. 3 differs from Fig. 2 because of the different detector setup, and that the large errors on high pulse-energy data in Fig. 3(b) are due to the lower event rate.

We next analyze quantitatively the DCH creation. The $K^h\alpha$-fluorescence counts may be given by

$$N_D = \frac{AF_D nP^2}{8\pi^{3/2} r_x r_y \Delta t} R\sigma^{(2)}, \tag{1}$$

where A is the efficiency of the spectrometer, F_D is the K-shell fluorescence yield for the DCH state, n is the number of atoms in the irradiated volume, P is the number of photons per pulse, r_x and r_y are the standard deviations of the Gaussian focus spot, and Δt is the pulse duration (standard deviations). We define the DCH cross section as that for a cw radiation by $\sigma^{(2)} = \sigma_N^{(1)} \tau_S \sigma_S^{(1)}$, where τ_S is the SCH lifetime, and $\sigma_N^{(1)}$ and $\sigma_S^{(1)}$ are the K-shell photoionization cross sections in the neutral and the SCH states, and introduce an effective cross section $R\sigma^{(2)}$, where R represents a correcting factor due to a pulsed and spiky temporal structure discussed below.

When the incident x rays are pulsed, the effective DCH cross section depends on τ_S as well as Δt. The DCH creation is described as sequential excitations by two x-ray photons [26]: the atom is excited to the SCH state at t, starts to decay with a lifetime of τ_S, and is excited at t' again to the DCH state. The whole process may be expressed as [27]

$$C = \frac{1}{2\pi\Delta t^2} \int_{-\infty}^{\infty} \sigma_N^{(1)} e^{(-t^2/2\Delta t^2)} \Big[\int_t^{\infty} \sigma_S^{(1)} e^{[-(t'-t)/\tau_S]} \times e^{(-t'^2/2\Delta t^2)} g^{(2)}(t'-t) dt' \Big] dt. \tag{2}$$

Here, the incident pulse is assumed to be a Gaussian with unit pulse energy, and $g^{(2)}(t)$ is the degree of the second-order coherence [28], which represents the spiky time structure of the self-amplified spontaneous-emission FEL in the present case.

First, we evaluate C for a single-mode pulse by setting $g^{(2)}(t) = 1$. In the limit of $\Delta t \gg \tau_S$, Eq. (2) can be integrated analytically, yielding $C_\infty = \sigma^{(2)}/\sqrt{\pi}\Delta t$. The correcting factor to $\sigma^{(2)}$ is defined as

$$R = C/C_\infty. \tag{3}$$

By introducing a normalized pulse duration $\xi = \sqrt{2}\Delta t/\tau_S$, Eq. (2) can be integrated numerically without losing generality. The pulsed effect is found to be negligible ($R \simeq 1$) for $\xi > 5$. Otherwise, the DCH creation is suppressed because the pulse finishes before the SCH state decays completely.

The spiky temporal structure is more important for R than the pulsed effect in the present case. The spikes make the instantaneous intensity higher than the average intensity and speed up the DCH creation. The experimental understanding of the coherence properties of the self-amplified spontaneous-emission FEL is still insufficient for our analysis. Here, we rely on numerical simulation and employ the SIMPLEX FEL simulation code [29], which reproduces well the lasing process of SACLA [2]. To perform reliable simulation, the degree of the first-order coherence [28] $g_{\rm exp}^{(1)}(t)$, calculated from measured spectra, was used to determine the electron beam parameters.

The spectra of the incident x rays shown in Fig. 4(a) were measured at 15 keV by a single-shot spectrometer with the Si 333 reflection [30]. The photon-energy resolution was 0.83 eV. Then, $g_{\rm exp}^{(1)}(t)$ was determined by the Fourier transform of the spectrum [31]

$$g_{\rm exp}^{(1)}(t) = \frac{\int_{-\infty}^{\infty} \langle I(\Delta\omega)\rangle \exp(i\Delta\omega t) d\Delta\omega}{\int_{-\infty}^{\infty} \langle I(\Delta\omega)\rangle d\Delta\omega}, \tag{4}$$

where $\langle I(\Delta\omega)\rangle$ is the ensemble average of the spectrum.

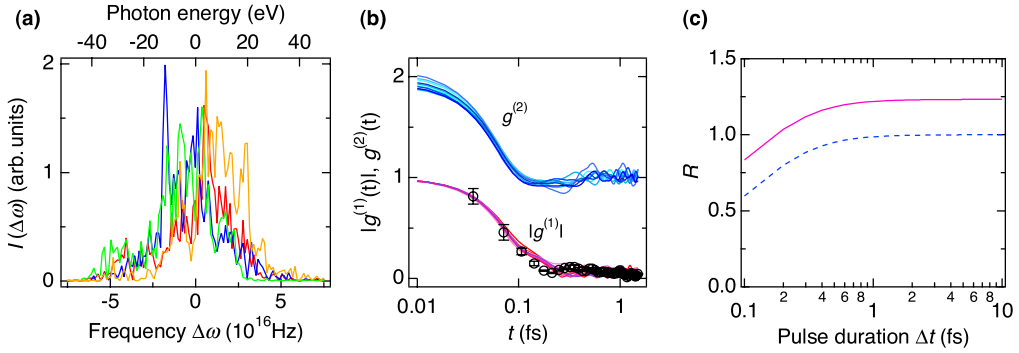

FIG. 4 (color online). Single-shot spectra, coherence functions, and correction due to spiky temporal structure. (a) Typical single-shot spectra at 15 keV. (b) The open circles show $|g_{\rm exp}^{(1)}(t)|$. The vertical bar indicates the statistical error. The lines show $|g_{\rm sim}^{(1)}(t)|$ and $|g_{\rm sim}^{(2)}(t)|$. (c) The correction factor R is plotted for $\tau_S = 170$ as. The solid line is calculated using the averaged $|g_{\rm sim}^{(2)}(t)|$. The dashed line for the single-mode radiation is shown for comparison.

The initial parameters of the electron beam, such as emittance and peak current, were determined from the FEL gain curve measured at 10 keV [2]. The degree of the first-order coherence $g^{(1)}_{\mathrm{sim}}(t)$ was calculated from the x-ray field obtained by the simulation. Then, the parameters were refined manually, so that $g^{(1)}_{\mathrm{sim}}(t)$ agrees with $g^{(1)}_{\mathrm{exp}}(t)$ as shown in Fig. 4(b). This refinement calibrates the temporal axis of the simulation because $g^{(1)}(t)$ and $g^{(2)}(t)$ relate to the temporal coherence of the field and the intensity, respectively. Finally, ten independent simulations were performed to determine $g^{(2)}_{\mathrm{sim}}(t)$ using the refined parameters. It is interesting to note that $g^{(1)}_{\mathrm{exp}}(t)$ is reproduced well by that expected for the chaotic radiation with the Gaussian spectrum $g^{(1)}(t) = \exp(-\pi t^2/2\tau_C)$, with a coherence time of $\tau_C = 97$ as in Refs. [28,31].

Equation (2) is integrated numerically for $\tau_S = 170$ as with $g^{(2)}_{\mathrm{sim}}(t)$, giving $R = 1.23$ for $\Delta t > 1$ fs [Fig. 4(c)]. The enhancement due to the spiky temporal structure is found to be small. The intensity fluctuation by the spikes is averaged out over the SCH lifetime because τ_C is only the half of τ_S. We perform our analysis based on the measured single-shot spectra for rigorous discussion; however, we consider that the bandwidth σ_ω is enough to determine $g^{(1)}(t)$ by $\tau_C = \sqrt{\pi}/\sigma_\omega$ [31].

Finally, we estimate the pulse duration using Eq. (1). This is possible due to the attosecond SCH lifetime, in spite of the fact that the DCH creation is a two-photon sequential process (Fig. 1). In contrast to the complex expression for N_D, the $K\alpha$-fluorescence counts may be given simply by $N_S = AF_S nP\sigma^{(1)}_N$, where F_S is the K-shell fluorescence yield in the SCH state. By combining this equation with Eq. (1) and approximating $F_S = F_D$ for krypton [32], the final expression for the pulse duration is deduced:

$$\Delta t = \frac{P}{8\pi^{3/2} r_x r_y} \frac{N_S}{N_D} \frac{R\sigma^{(2)}}{\sigma^{(1)}_N}. \tag{5}$$

The magnitude of $\sigma^{(2)}$ is still controversial, and two independent calculations are applied to the following analysis. First, we use $\sigma^{(1)}_N = 1.69 \times 10^{-20}$ cm^2 [33] and $\tau_S = 170$ as, and estimate $\sigma^{(2)} = 2.4 \times 10^{-56}$ cm^4 s. Here, $\sigma^{(1)}_S$ is approximated by $\sigma^{(1)}_N/2$. The factor of $1/2$ represents only one K electron remaining in the SCH state. In the second calculation, the Los Alamos National Laboratory Atomic Physics Codes [34] are employed: $\sigma^{(1)}_N = 1.43 \times 10^{-20}$ cm^2, $\sigma^{(1)}_S = 7.39 \times 10^{-21}$ cm^2, and $\sigma^{(2)} = 1.8 \times 10^{-56}$ cm^4 s.

The $K^h\alpha$-to-$K\alpha$ ratio is estimated to be $N_D/N_S = (3.95 \pm 0.17) \times 10^{-4}$ from the spectrum measured with the intense pulses (Fig. 2). This allows us to determine the pulse duration to be 2.5–2.8 fs (FWHM) at 15 keV. The peak intensity at the focus is $(1.5\text{–}1.7) \times 10^{18}$ W/cm^2, or equivalently $(6.3\text{–}7.1) \times 10^{32}$ photons/cm^2 s. The range of estimation is due to the two independent values of $\sigma^{(2)}$. The estimation is consistent with the electron bunch length of 2.4 fs (FWHM) deduced from the measured FEL gain length [35] in consideration of the slippage length [31], which confirms the validity of our analysis.

In summary, we show experimentally that the SCH atoms with a 170-as lifetime partially scatter x rays at a peak intensity of 10^{18} W/cm^2. When we extrapolate simply from the present result, the x-ray scattering by SCH atoms would reach a few percent of that by neutral atoms at 10^{20} W/cm^2 and would be detectable in a wide variety of experiments. For example, when x-ray FEL is focused tightly on a nanocrystal with a size of 100 nm, the peak intensity reaches 10^{20} W/cm^2 or more, and the scattering by the SCH atoms can affect the diffraction patterns. The shot-to-shot fluctuation of the peak intensity prevents normalizing the diffraction intensities due to the nonlinearity, which might be serious for the anomalous phasing. Since the fluorescence spectrum gives the population of the SCH atoms scattering x rays, simultaneous measurement of the fluorescence spectrum and the diffraction data of standard crystals could be used to extract the structure factor in the SCH state and to investigate the anomalous phasing under intense x-ray irradiation.

We show that the quantitative analysis of the DCH creation can give a simple estimation of the pulse duration in the sub-10-fs range. Because of the higher efficiency compared to second-harmonic generation and two-photon absorption, the DCH creation is considered to be a promising process for developing an x-ray autocorrelator. The DCH spectroscopy combined with a femtosecond optical delay enables characterization of the pulse shape [36] without the exact knowledge of $\sigma^{(2)}$ and $g^{(2)}(t)$.

We are grateful to T. Kumasaka and H. Tanaka for fruitful discussions and J. Harries for helpful comments and critical reading of the manuscript. This work was supported by JSPS KAKENHI (23360038). The experiments were performed with the approval of JASRI (Proposal No. 2012A8025).

*tamasaku@riken.jp
†Deceased.

[1] P. Emma *et al.*, Nat. Photonics **4**, 641 (2010).
[2] T. Ishikawa *et al.*, Nat. Photonics **6**, 540 (2012).
[3] R. Neutze, R. Wouts, D. van der Spoel, E. Weckert, and J. Hajdu, Nature (London) **406**, 752 (2000).
[4] H. N. Chapman *et al.*, Nature (London) **470**, 73 (2011).
[5] J. Kern *et al.*, Proc. Natl. Acad. Sci. U.S.A. **109**, 9721 (2012).
[6] S. Boutet *et al.*, Science **337**, 362 (2012).
[7] L. Young *et al.*, Nature (London) **466**, 56 (2010).
[8] G. Doumy *et al.*, Phys. Rev. Lett. **106**, 083002 (2011).
[9] S.-K. Son, L. Young, and R. Santra, Phys. Rev. A **83**, 033402 (2011).

[10] U. Lorenz, N. M. Kabachnik, E. Weckert, and I. A. Vartanyants, Phys. Rev. E **86**, 051911 (2012).
[11] S.-K. Son, H. N. Chapman, and R. Santra, Phys. Rev. Lett. **107**, 218102 (2011).
[12] W. A. Hendrickson, Science **254**, 51 (1991).
[13] L. Fang *et al.*, Phys. Rev. Lett. **105**, 083005 (2010).
[14] N. Berrah *et al.*, Proc. Natl. Acad. Sci. U.S.A. **108**, 16 912 (2011).
[15] W. A. Hendrickson, J. R. Horton, and D. M. LeMaster, EMBO J. **9**, 1665 (1990).
[16] H. Yumoto *et al.*, Nat. Photonics **7**, 43 (2013).
[17] J. Niskanen, P. Norman, H. Aksela, and H. Ågren, J. Chem. Phys. **135**, 054310 (2011).
[18] R. W. Dunford, E. P. Kanter, B. Krässig, S. H. Southworth, and L. Young, Radiat. Phys. Chem. **70**, 149 (2004).
[19] M. O. Krause and J. H. Oliver, J. Phys. Chem. Ref. Data **8**, 329 (1979).
[20] M. H. Chen, B. Crasemann, and H. Mark, Phys. Rev. A **25**, 391 (1982).
[21] R. Diamant, S. Huotari, K. Hämäläinen, R. Sharon, C. Kao, and M. Deutsch, Phys. Rev. A **79**, 062511 (2009).
[22] M. M. Hall, J. Appl. Crystallogr. **10**, 66 (1977).
[23] A. M. Costa, M. C. Martins, J. P. Santos, P. Indelicato, and F. Parente, J. Phys. B **40**, 57 (2007).
[24] K.-I. Hino, T. Ishihara, F. Shimizu, N. Toshima, and J. H. McGuire, Phys. Rev. A **48**, 1271 (1993).
[25] Y. Hikosaka, P. Lablanquie, F. Penent, T. Kaneyasu, E. Shigemasa, J. Eland, T. Aoto, and K. Ito, Phys. Rev. Lett. **98**, 183002 (2007).
[26] No $K^h\alpha$ signal was observed for a 14.7-keV pump, which forbids P_2 (Fig. 1) and allows only direct two-photon DCH creation, indicating that the sequential process is dominant in the present study.
[27] N. Rohringer and R. Santra, Phys. Rev. A **76**, 033416 (2007).
[28] R. Loudon, *The Quantum Theory of Light* (Oxford University Press, Oxford, England, 1983).
[29] T. Tanaka, *Proceedings of the 2004 FEL Conference* (Comitato Conferenze Elettra, Trieste, 2004), p. 435.
[30] Y. Inubushi *et al.*, Phys. Rev. Lett. **109**, 144801 (2012).
[31] E. L. Saldin, E. A. Schneidmiller, and M. V. Yurkov, *The Physics of Free Electron Lasers* (Springer, Berlin, 2000).
[32] M. H. Chen, Phys. Rev. A **44**, 239 (1991).
[33] W. J. Veigele, At. Data Nucl. Data Tables **5**, 51 (1973).
[34] Los Alamos National Laboratory Atomic Physics Codes, http://aphysics2.lanl.gov/tempweb/.
[35] T. Tanaka *et al.*, *Proceedings of the 9th Annual Meeting of Particle Accelerator Society of Japan* (Particle Accelerator Society of Japan, Tokyo, 2012), p. 54.
[36] A. Gutierrez, P. Dorn, J. Zeller, D. King, L. F. Lester, W. Rudolph, and M. Sheik-Bahae, Opt. Lett. **24**, 1175 (1999).